Modeling and simulation of the QUENCH 12 experiment with the RELAP/SCDAPSIM/MOD3.5 code

Gergana Gerova, Ivan Spasov, Chris Allison, and Martin Steinbrück

Citation: AIP Conference Proceedings **2048**, 020019 (2018); doi: 10.1063/1.5082037
View online: https://doi.org/10.1063/1.5082037
View Table of Contents: http://aip.scitation.org/toc/apc/2048/1
Published by the American Institute of Physics

Modeling and Simulation of the QUENCH 12 Experiment with the RELAP/SCDAPSIM/MOD3.5 Code

Gergana Gerova[1,a)], Ivan Spasov[1,2,b)], Chris Allison[3,c)], Martin Steinbrück[4,d)]

[1]*Technical University of Sofia*
Faculty of Power Engineering and Power Machines
Department of Thermal and Nuclear Power Engineering
8, Kl.Ohridski Blvd., 1000 Sofia, Bulgaria

[2]*Institute for Nuclear Research and Nuclear Energy*
Bulgarian Academy of Sciences,
72 Tzarigradsko Shosse Blvd., 1000 Sofia, Bulgaria

[3]*Inovative Systems Software LLC*
3585 Briar Creek Ln. Ammon, ID 834066, USA

[4]*Karlsruhe Institute of Technology*
Institute for Applied Materials – Applied Materials Physics
Hermann-von-Helmholtz-Platz 1
76344 Eggenstein-Leopoldshafen, Germany

[a)] ggg@tu-sofia.bg
[b)] spasov@tu-sofia.bg, spasov@inrne.bas.bg
[c)] issgml97@gmail.com
[d)] martin.steinbrueck@kit.edu

Abstract. This paper presents a RELAP/SCDAPSIM MOD3.5 model of the QUENCH 12 experiment. The model uses the new heater rod model and automatic time advancement in the simulation of experiment and it is based on the basis Innovative Systems Software's input deck with 22 axial nodes.

INTRODUCTION

Reliable and safe operation of nuclear power plants (NPPs) is paramount. Therefore, the behavior of NPPs' systems as well as fuel and surrounding materials from thermal-hydraulic, physicochemical, and mechanical point of view during any accidents must be known in order to design adequate accident mitigation measures.

The most important of accident management and mitigation measures is the termination of transients and/or sequence of events which could lead to severe accidents in Light Water Reactors. This is achieved by water injection into the uncovered overheated core of a nuclear reactor. Analyses that were performed after the Three Mile Island accident and results of different in-pile and out-of-pile experiments have shown that in some cases right before water succeeds in cooling the core there could be sharp temperature increase, hydrogen production and fission products

Proceedings of the 44th International Conference on Applications of Mathematics in Engineering and Economics
AIP Conf. Proc. 2048, 020019-1–020019-15; https://doi.org/10.1063/1.5082037
Published by AIP Publishing. 978-0-7354-1774-8/$30.00

release. All of these phenomena are caused by enhanced oxidation of zirconium alloy claddings [1, 2]. The reasons for this enhanced oxidation are not yet fully understood. Initially it was thought that the cracking of oxide layers due to the thermal shock and subsequent exposure of fresh Zircaloy to steam are significant factors [3]; but currently it is believed that all processes should be taken into account affecting, on the one hand, the cooling of the core and, on the other hand, the oxidation kinetics [4].

It is very important that the fuel cladding maintains its integrity in a postulated design based accidents such as a loss-of-coolant-accident (LOCA). During a LOCA event, the fuel cladding is faced to ballooning, high temperature oxidation, hydration uptake/hydriding, and creep which are the most important unfavorable effects as well as it is quenched by water due to the action of the emergency core cooling systems. Under these conditions fuel claddings degrading their properties and creep cause tube deformation and texture changes in the alloy. So it is necessary that the fuel claddings to preserve their mechanical, structural, and chemical properties during various types of accidental conditions [5-10].

Furthermore, water injection into the uncovered overheated core (quenching) is considered the worst case accidental scenario regarding hydrogen release in the containment. Significant hydrogen generation due to zirconium-steam reaction occurs when the core temperature exceeds 1000 K. This fact is of high importance when different safety analyses are carried out since it is necessary to prove that hydrogen production rates and its total amount should not exceed certain safety limits. When the hydrogen amount is known in advance then there is a possibility to design adequate measures to mitigate the effects of accidents that may occur due to its presence.

One of the purposes of experiments like QUENCH, CORA, PHEBUS FP is the determination of physical and chemical phenomena related to hydrogen generation due to quenching phase. So far this issue cannot be completely clarified on the basis of currently available Zircaloy-Steam oxidation correlations. On the other hand, there are no sophisticated models available capable to predict correctly the thermal-hydraulic and cladding behavior especially during quenching phases [1].

The QUENCH Program was launched in 1996 at Karlsruhe Institute of Technology (former Forschungszentrum Karlsruhe). The Program's goal is investigating the hydrogen source term resulting from water injection into a LWRuncovered core of [1] and different cladding materials' behavior [4, 11,12,13]. Furthermore, QUENCH tests play an important role in validation of different computer codes by creating database for model development and codes' improvements [14].

The objective of the present work is to create and test computational RELAP/SCDAPSIM MOD3.5 model using the new heater rod model [15,16]and automatic time advancement in simulation of the QUENCH-12 experiment. The numerical uncertainties due to different discretization as well as numerical schemesare not subject of this study.

QUENCH-12 TEST AND BUNDLE CHARACTERISTICS

QUENCH-12 was conducted at the Karlsruhe Institute of Technology on 27 September 2006 in the frame of the EC-supported ISTC program 1648.2. The experiment was proposed by KIT, RIAR Dimitrovgrad and IBRAE Moscow (Russia), supported by pretest calculations performed by PSI (Switzerland), the Kurchatov Institute Moscow (Russia), and IRSN Cadarache (France) [1, 12,13,17,18].

The QUENCH-12 test bundle is set-up to investigate the effects of VVER materials (niobium-bearing zirconium alloys) and bundle geometry (hexagonal lattice) under core reflood conditions. The QUENCH-06 test (ISP-45) with PWR materials (Zr-4 claddings) and geometry (square lattice) is chosen as a benchmark. QUENCH-12 is conducted with largely the same protocol as QUENCH-06, so that the effects of VVER characteristics could be observed more easily [1, 14, 17, 19, 20].

Full design characteristics of the QUENCH-06 (PWR) and the QUENCH-12 (VVER) test bundles are given in detail in [1, 21, 22].

The QUENCH-12 test bundle is approximately 2.5 m long and consists of 18 heated and 13 unheated fuel rod simulators. The total heating power is distributed between the two groups of heated rods as follows: 33% of the power is used for six inner ring fuel rod simulators and the remaining 67%in the twelve outer ring rod simulators. The simulators are held in their locations by seven grid spacers made of Zr1%Nb. The simulators' claddings are the same as those used in VVERs with respect to material and dimensions. Heated rods are filled with Ar5%Kr while unheated ones with He. The different fill gases allow observation of a first cladding failure which then can be distinguished between heated and unheated test rods. The bundle is equipped with six Zr1%Nb corner rods. Three of them are used for thermocouple instrumentation while the remaining three could be withdrawn from the bundle for checking the amounts of ZrO_2 oxidation and hydrogen uptake at pre-defined times [1, 13, 14, 17, 18, 20, 23].

Fig. 1 shows test phases during the QUENCH-12 experiment.

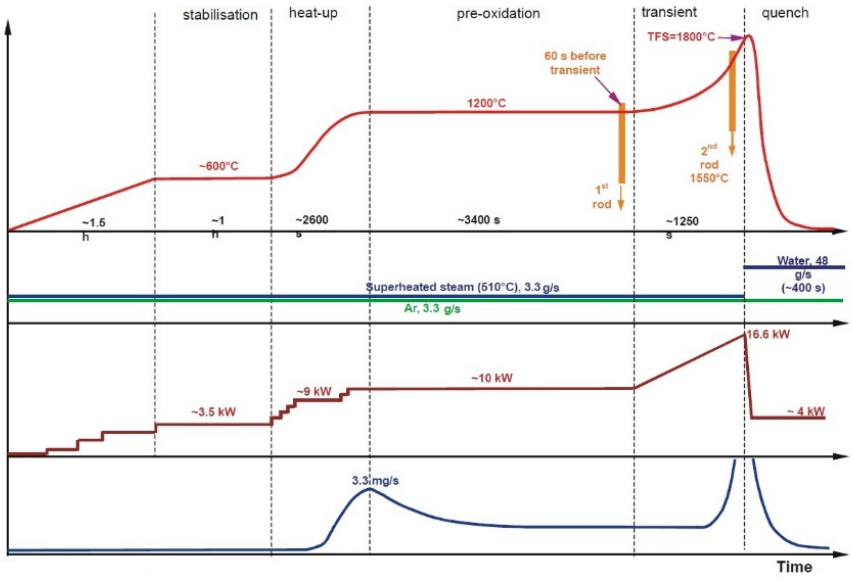

FIGURE 1. Test phases [1, 13]

The test starts with application of electrical power of 3.5 kW which is ramped step-wise to 9.9 kW over ~ 2300 s in order to reach the desired pre-oxidation temperature of 1473 K in a flow of 3.3 g/s argon and 3.3 g/s steam and to achieve target cladding oxidation of around 200 μm. The pre-oxidation phase continued until the test time of 6000 s. At about this time corner rod D is withdrawn to check the oxidation level. The power is then ramped at a rate of 5.1 W/s to cause a temperature increase until the desired maximum temperature before quench of 2073 K is reached. Corner rod F was withdrawn after about 900 s from the start of the transient phase, when the bundle temperature is about 1823 K at the 950 mm level. Reflood with 48 g/s of water is initiated and the electrical power is reduced to 4 kW simulating effective decay heat levels. The temperatures at elevations between 850 mm and 1050 exceed the melting temperature of β-Zr, i.e. 2033 K. The third corner rod, i.e. rod "B" is withdrawn after the test with the same intention – to check oxide levels and hydrogen absorption. All of the three corner rods exhibit strong spalling of oxide scales or so called breakaway oxidation effects [1, 13, 14, 18, 23].

The total hydrogen generated by the test is 58 g (QUENCH-06: 36 g). During reflood 24 g of hydrogen are generated (QUENCH-06: 4g) [1,14,20]. Increased hydrogen generation rate in QUENCH-12 test in comparison with QUENCH-06 is generally due to extensive cladding surface failure related to breakaway oxidation and local melt formation with subsequent melt oxidation. The possible sources of increased hydrogen production can be summarized as: 1) interaction between steam and new metal surfaces appeared by spalling of oxide scales damaged because of the breakaway effect; 2) release of hydrogen absorbed in metal by breakaway; 3) moderate melt oxidation released into the space between rods [13, 14, 18, 19].

The term *breakaway* stands here for the loss of protectiveness of an oxide scale due to its mechanical failure and consequently the transition to a faster oxidation kinetics. An additional safety impact of intensive breakaway oxidation may arise due to the associated accelerated hydrogen uptake and consequent material embrittlement of the E110 claddings and the E125 bundle shroud. This can lead to severe degradation of the bundle during quenching [18].

Due to pronounced breakaway oxidation over large areas in the bundle, (1) significantly more hydrogen is absorbed during pre-quench phases in QUENCH-12 (10 g, in comparison to 2 g in QUENCH-06), and (2) significantly more hydrogen is released during quench. The axial distribution of hydrogen concentration in the metal is strongly correlated with the oxide scale morphology.

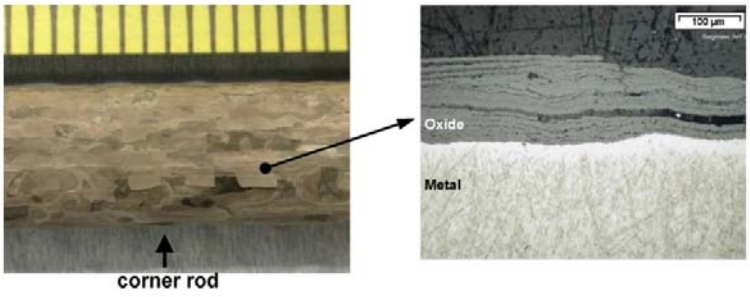

FIGURE 2. Breakaway oxidation in the QUENCH-12 bundlewith E110 corner rods [4]

The higher amount of hydrogen released during the quench phase of the QUENCH-12 bundle can be explained by pre-damaged oxide layers, melt oxidation, and release of previously absorbed hydrogen. Post-test examinations of the bundle show distinct spalling and relocation of oxide scales for the QUENCH-12 bundle as shown in Fig. 2. [4]

The breakaway effect is observed also for the Zyrcaloy-4 alloy but with less intensity than for the niobium-bearing alloys (E110 and E125). The temperature range between 1020 and 1370 K is typical for the development of breakaway oxidation of the E110 alloy, whereas breakaway of Zircaloy-4 occurs later and in a narrower temperature range [18].

Generally, the oxidation of zirconium alloys is strongly dependent on composition and boundary conditions, like oxidizing atmosphere, as soon as breakaway starts [11].

The cladding integrity is considerably decreased after the breakaway oxidation because of the steep increase of oxide thickness and hydrogen pickup by the breakaway oxidation. The oxide structure is mainly considered as an important factor to explain the breakaway oxidation kinetics of zirconium claddings because the phase transformation between tetragonal and monoclinic oxide imposes on the formation of cracks and pores in the oxide layer [5, 10].

The introduction of new cladding materials for the fuel rods of nuclear reactors should also demand a standard method for the evaluation of ductile-to-brittle transition under LOCA conditions. The more so, several experiments have indicated significant differences in the oxidation kinetics and the mechanical behavior between different Zirconium alloys at high temperature. For this reason, specific LOCA criteria should be identified for each cladding material. [7].

CODE USED FOR THE ANALYSIS

Based on the post-test calculations of the QUENCH experiments, the capability of the best estimate codes can be established and evaluated [24–28]. Here this is done by means of Reactor Excursions and Leak Analysis Program/Severe Core Damage Analysis Package Innovative Systems Software (RELAP/SCDAPSIM). The RELAP/SCDAPSIM code is being developed as part of an international nuclear technology development program called SDTP [29]. It is designed to predict the overall reactor coolant system thermal hydraulic response and core behavior during normal operational conditions as well as under design basis or severe accident conditions [28, 30, 31]. RELAP/SCDAPSIM uses the publicly available RELAP/MOD3.3 as well as SCDAP/RELAP5/MOD3.2 models developed by the US Nuclear Regulatory Commission (NRC) in a combination with proprietary advanced programing and numerical methods, user options, and models developed in frame of the International SCDAP Development and Training Program (SDTP) [28, 30, 32].

The administrator for the SDTP program and main developer of specific models for the RELAP/SCDAPSIM is a private, limited liability company Innovative Systems Software (ISS) and their enhancements allow the code to run faster and more reliable than the original US NRC codes [30].

In RELAP/SCDAPSIM/MOD3.5 the overall thermal hydraulics of the reactor coolant system, control system behavior, reactor kinetic as well as behavior of several special reactor system components such as valves and pumps are being calculated by the RELAP5 part of the code and its models [33]. On the other hand, the behavior of the core and vessel structures under normal as well as accident conditions is being calculated by SCDAP.

The RELAP5 hydrodynamic model is a one-dimensional, transient, two-fluid model for flow of two-phase steam-water mixture that can contain non-condensable components in the steam phase and/or a soluble component in the water phase. The equations of motion (1 – 6) are formulated in terms of volume and time-averaged parameters of flow [33].

The continuity equations are:

$$\frac{\partial}{\partial t}\left(\alpha_g \rho_g\right)+\frac{1}{A}\frac{\partial}{\partial x}\left(\alpha_g \rho_g v_g A\right)=\Gamma_g \tag{1}$$

$$\frac{\partial}{\partial t}\left(\alpha_f \rho_f\right)+\frac{1}{A}\frac{\partial}{\partial x}\left(\alpha_f \rho_f v_f A\right)=\Gamma_f \tag{2}$$

The momentum equations for vapor and liquid phase are as follow:

$$\begin{aligned}&\alpha_g\rho_g A\frac{\partial v_g}{\partial t}+\frac{1}{2}\alpha_g \rho_g A\frac{\partial v_g^2}{\partial x}=\\ =&-\alpha_g A\frac{\partial P}{\partial x}+\alpha_g\rho_g B_x A-\left(\alpha_g\rho_g A\right)FWG\left(v_g\right)+\Gamma_g A\left(v_{gI}-v_g\right)-\left(\alpha_g\rho_g A\right)FIG\left(v_g-v_f\right)-\\ &-C\alpha_g\alpha_f\rho_m A\left[\frac{\partial\left(v_g-v_f\right)}{\partial t}+v_f\frac{\partial v_g}{\partial_x}-v_g\frac{\partial v_f}{\partial_x}\right]\end{aligned} \tag{3}$$

$$\begin{aligned}&\alpha_f \rho_f A\frac{\partial v_f}{\partial t}+\frac{1}{2}\alpha_f\rho_f A\frac{\partial v_f^2}{\partial x}=\\ =&-\alpha_f A\frac{\partial P}{\partial x}+\alpha_f\rho_f B_x A-\left(\alpha_f\rho_f A\right)FWG\left(v_f\right)+\Gamma_g A\left(v_{fI}-v_f\right)-\left(\alpha_f\rho_f A\right)FIG\left(v_f-v_g\right)-\\ &-C\alpha_f\alpha_g\rho_m A\left[\frac{\partial\left(v_f-v_g\right)}{\partial t}+v_g\frac{\partial v_f}{\partial_x}-v_f\frac{\partial v_g}{\partial_x}\right]\end{aligned} \tag{4}$$

The thermal energy equations are:

$$\frac{\partial}{\partial t}\left(\alpha_g\rho_g U_g\right)+\frac{1}{A}\frac{\partial}{\partial x}\left(\alpha_g\rho_g U_g v_g A\right)=-P\frac{\partial\alpha_g}{\partial t}-\frac{P}{A}\frac{\partial}{\partial x}\left(\alpha_g v_g A\right)+Q_{wg}+Q_{ig}+\Gamma_{ig}h_g^*+\Gamma_w h_g^{'}+DISS_g \tag{5}$$

$$\frac{\partial}{\partial t}\left(\alpha_f\rho_f U_f\right)+\frac{1}{A}\frac{\partial}{\partial x}\left(\alpha_f\rho_f U_f v_f A\right)=-P\frac{\partial\alpha_f}{\partial t}-\frac{P}{A}\frac{\partial}{\partial x}\left(\alpha_f v_f A\right)+Q_{wf}+Q_{if}+\Gamma_{ig}h_f^*+\Gamma_w h_f^{'}+DISS_f \tag{6}$$

where:

- A – cross-sectional area (m^2);
- P – pressure (Pa);
- U_g, U_f –specific internal energies for vapor and liquid phases (J/kg);
- α_g, α_f – vapor and liquid volume fraction;
- v_g, v_f – velocities for vapor and liquid phases (m/s);
- ρ_g, ρ_f – density for vapor and liquid phases (kg/m^3);
- ρ_m – density of two-phase mixture (kg/m^3);

- t –time (s);
- x – distance (m);
- Γ_g, Γ_f – volumetric mass exchange rate for vapor and liquid phase (kg/m^{3}s);
- Γ_{gl} – mass transfer at the vapor/liquid interface in the bulk fluid (kg/m^{3}s);
- Γ_w – mass transfer at the vapor/liquid interface in the boundary layer near the walls (kg/m^{3}s);
- FIG, FIF – interfacial friction coefficients for vapor and liquid phases (s^{-1});
- $DISS_g, DISS_f$ – energy dissipation for vapor and liquid phases (W/m^3);
- FWG, FWF – wall drag coefficients for vapor and liquid phase (s^{-1});
- B_x – body force in x coordinate direction (m/s^2);
- C – coefficient of virtual mass;
- Q_{wg}, Q_{wf} – phasic wall heat transfer rate per unit volume (W/m^3);
- Q_{ig}, Q_{if} – phasic interface heat transfer terms (W/m^3);
- h_g^*, h_f^* – phasic enthalpies associated with bulk interface mass transfer (J/kg);
- $h_g^{'}, h_f^{'}$ – phasic enthalpies associated with wall interface mass transfer (J/kg).

The system model can be solved numerically using semi-implicit or nearly-implicit finite difference technique.

SCDAP is the part of code that includes user-selectable reactor component models for LWR fuel rods, Ag-In-Cd and B_4C control rods, BWR control blade/channel boxes as well as electrically heated fuel rod simulators, general vessel and core structures. SCDAP also has models to treat the later stages of severe accidents with debris and molten pool formation, debris/vessel interactions and the structural failure (creep rupture) of vessel structures [31, 32, 34].The code uses two-dimensional heat conduction model(equation 7) for the core components and parabolic rate (equation 8) for the material oxidation.

$$\int_V \rho c_p \frac{\partial T}{\partial t} dV = \int_V \frac{1}{r} \frac{\partial}{\partial r}\left(rk \frac{\partial T}{\partial r} \right) dV + \int_V \frac{\partial}{\partial z}\left(k \frac{\partial T}{\partial z} \right) dV + \int_V Q_v dV + \int_S Q_s dS \tag{7}$$

where:

- Q_V – volumetric heat source (W/m^3);
- Q_S – surface heat flux (W/m^2);
- T – temperature at location (r, z) at time t where r and z are the radial and axial coordinates;
- c_p – volumetric heat capacity (J/m^{3}K);
- k – thermal conductivity (W/m.K).

$$\frac{d\delta}{dt} = \frac{A}{\delta} e^{\left(-\frac{B}{T}\right)} \tag{8}$$

where:

- δ – weight gain or layer thickness (kg/m^2 or m);
- T – temperature (K);
- t – time (s);
- A, B –constants.

MODELING ASSUMPTIONS

A QUENCH 12 model based on the basis Innovative Systems Software's input deck with 22 axial nodes [33] is created. The electric heaters, simulators of fuel rods, corner rods, and shroud are represented using SCDAP components. The new heater rod model (*wolfhn*) [15, 16] is applied. It takes into account the actual heater rod

structure and consists of tungsten heating element, inner gas-filled gap, ZrO_2 pellets, outer gas-filled gap, and cladding. The rod is described by thirteen radial rings: 3 for the tungsten heater, 1 for the inner gap, 3 for the ZrO_2pellets, 1 for the outer gap, and 5 rings for the cladding. The conductivity increase in case of gap closure is not taken into account. The thickness of the annular ZrO_2 pellet is 1 mm smaller than that used in the experiment.

The mathematical models of new heater rod model [15, 16] are given below:

$$P_{(i)} = \frac{R_{(i)}}{R_{total}} \frac{P_{total}}{z_{(i)}} \tag{9}$$

Here P_{total} is the total input power, $P_{(i)}$ is the power per unit length, R_{total} is the total electrical resistance, $R_{(i)}$ is the electrical resistance per unit length, and $z_{(i)}$ is the node length.

The total electrical resistance is obtained as follows:

$$R_{total} = R_{stat} + \sum_{i=1}^{N} R_{(i)} \tag{10}$$

where R_{stat} is the static electrical resistance.

The electrical resistance per unit length is calculated as:

$$R_{(i)} = \rho_{(W,Mo,Cu)}(T) \frac{\delta z}{A_{wire}\left(1+\beta(T)\right)} \tag{11}$$

where following notations are used:

- A_{wire} – nodal cross section area, mm^2;
- δz – nodal length, m;
- T – rod temperature, K;
- $\rho_{(W,Mo,Cu)}(T)$ – the specific resistance of the materials, $\Omega.mm^2/m$;
- $\beta(T)$ – the thermal expansion coefficient.

$$\rho_W(T) = -2.61*10^{-2} + 2.63*10^{-4}*T + 2.20*10^{-8}*T^2 \tag{12}$$

$$\rho_{Mo}(T) = 2.249*10^{-2} + 5.36*10^{-5}*T + 1.38*10^{-7}*T^2 - 2.22*10^{-11}*T^3 \tag{13}$$

$$\rho_{Cu}(T) = -7.89*10^{-3} + 9.90*10^{-5}*T - 5.49*10^{-8}*T^2 + 3.16*10^{-11}*T^3 \tag{14}$$

Here the temperature T is in K and specific resistivity in $\Omega.mm^2/m$.

The nodalization scheme of the test section is shown in Fig. 3.It has thirty-one axial nodes.The heated part of the components is represented by 20 axial nodes with a length 0.05 m each. Spacer grids are taken into account in SCDAP model. The central unheated rod is modeled as "fuel rod" component. It is composed of UO_2 pellets in the center, a gas filled gap and a Zr1%Nb cladding. The UO_2 pellets are represented by 3 radial nodes, the gas gap by a node, and the cladding by 9 radial nodes. The six heated rods located around the central unheated rod are modeled by means of simulator component with electrical resistance equal to 2.1 mΩ. The second ring formed by 12 unheated rods is performed as a "fuel" rod component. The same radial discretization is used as for the central unheated rod. The twelve outer heaters are represented by means of a "simulator" component, which is used for modeling of electrically heated rods. The electrical resistance equal to 3.0 mΩ is defined. Corner rods are formed by "fuel" rod component. It has the following radial nodes: 1 for UO_2, 1 for the gas gap and 9 for the cladding. The "shroud" component is used for modeling the shroud of the bundle. It consists of inner Zr2.5Nb layer, ZrO_2insulation layer and a stainless steel layer. The inner layer made by Zirconium alloy is modeled by a radial ring. One radial node is applied for the insulator layer and 3 for the stainless steel.

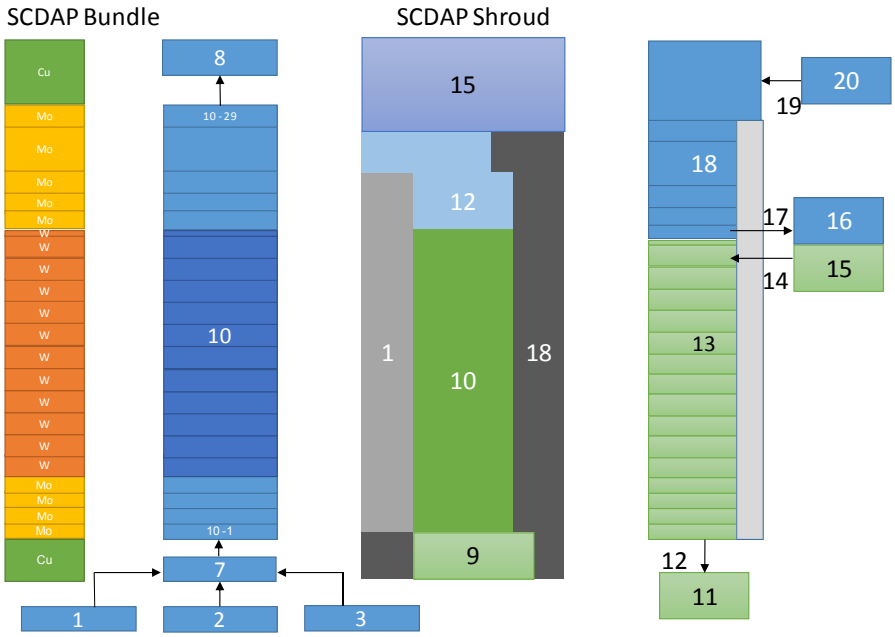

FIGURE 3. Nodalization scheme of the QUENCH 12 test section

The space of the test section, which is filled with superheated steam and argon, is described by RELAP5 components. The inlet boundary conditions are defined by time-dependent components “001”, “003” and “005” as well as by time-dependent junctions “002”, “004” and “006”. The lower plenum has length 0.15 m and is represented by branch component “007”.The hydraulic part of the bundle is modeled by pipe component “010”. It has the same axial nodalization as the corresponding part of the SCDAP components. The spacer grids are not modeled explicitly. They are taken into account by pressure loss coefficients equal to 0.001. Additional pressure loss coefficients are not used. The outlet boundary conditions for the hydraulic part of the test section are defined in time-dependent component “008”.

The argon cooling jacket is modeled by pipe component “013”. It has the following axial discretization:

- 4 nodes with length 0.075 m each representing the section lower than the heated part of facility;
- 18uniform nodes with length 0.05 m, one node with length 0.049 m and a node with 0.075 m for the heated length of the test section.

The water part of the cooling jacket is given by pipe component “018”. It is divided into six nodes with different axial length.

RELAP5 heat structure with 5 radial points is applied for the Inconel layer of the cooling jacket.

Calculation with automatic time advancement is applied. The algorithm for time advancement uses semi-implicit scheme when the time step is below the Courant limit and nearly implicit when the large time step is taken [35].

The Kurchatov Institute’s modification of the MATPRO libraries for niobium containing cladding material is used.

The shattering oxidation model is used. For oxidation in steam environment Sokolov’s model is applied. User defined properties are used for argon and ZrO_2. They are taken from the basic ISS QUENCH 06 input deck developed by H. Madokoro [15] and refer to case with the properties given by the manufacturer.

RESULTS

The results show good agreement with the measured temperatures in the lower part of the test section. Up to the quench phase, there is a maximum deviation of about 100 ˚C for the simulator rods, and about 150 ˚C for the shroud. The comparison between the measured and calculated outer surface shroud temperature at elevation 650 mm is given in Fig. 4. The predicted temperature is depicted in blue, the temperature of TSH 10/90 thermocouple is shown in red and TSH 10/270 is green. A difference of about 170 ˚C is observed at the beginning of the pre-oxidation phase, which decreases to about 100 ˚C during the transient. Excellent similarity is illustrated in the quench phase,

where the shroud is cooled with a delay of 30 seconds. Such temperature behavior is seen, up to and including elevation 750 mm.After that, the temperature difference between the calculated and the measured values increases, and its maximum being at the elevation 1050 mm.

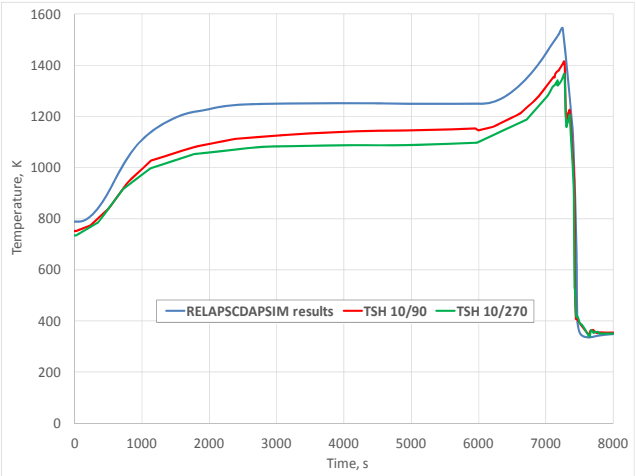

FIGURE 4. Time history of the measured and calculated outer shroud surface temperatures at elevation 650 mm

The outcomes for elevation 950 mm are presented in Fig. 5 through Fig. 10. In the pre-oxidation phase between 3500 and 4500 seconds are noticed some temperature variations (Fig. 5), which occur only at this level. The observed effect can't be distinguished clearly. It can be a consequence of the zirconium oxide transition from monoclinic to tetragonal structure in the oxide film by oxidizing at 1600 K resulting in an increase in specific heat capacity [36] or due to computational effects.

Fig. 5 and Fig. 6 present inner unheated rod central line and outer surface temperatures, in comparison with the thermocouples measurements. A good agreement with the measured data is displayed. Similar, to the observations made in [37], there is an under-prediction of radial heat losses in the upper test section. As a result of the computed higher cladding temperature during the heat-up and pre-oxidation phases, the material phase transition temperature is reached more rapidly (which for the Sokolov's correlation is 1773 K). This in turn leads to subsequent oxidation kinetics acceleration and higher temperatures prediction. The deviation between the maximum measured and calculated inner unheated rod temperatures is about 310 ˚C.

The time history of the calculated and measured outer heated rod surface temperature at elevation 950 mm is illustrated in Fig. 7. The model reproduced qualitatively the temperature change. It provides a maximum cladding temperature higher by 105 ˚C.

The computed cladding surface and the center line temperature change of the outer unheated rod at elevation 950mm during the transient and quench phases are shown in Fig. 8 and Fig. 9. The results are in agreement with the measured temperatures during quench phase. The deviation between the predicted maximum temperature and the measured one by thermocouple TFSU 10/4/13, which is located on the surface of the fuel rod simulator 10 group 4 is about 195 ˚C. The difference decreases to about 150 ˚C compared to the TFSU 17/3/13 data. The thermocouple is set on the fuel rod simulator 17, which is placed at group 3.

The excellent accordance between the predicted and measured shroud temperatures is depicted in Fig. 10. The deviation between the maximum predicted temperature and the measured TSH 13/90 value is about 15 ˚C. The comparison of the other thermocouple (TSH 13/270) gives a difference of 170 ˚C.

The time history of the shroud surface temperature at elevation 1150 mm is presented in Fig. 11.

Fig. 12 shows the integral hydrogen production. The model overestimates the amount of generated hydrogen by 37 grams, which is with 64% higher than the measured.

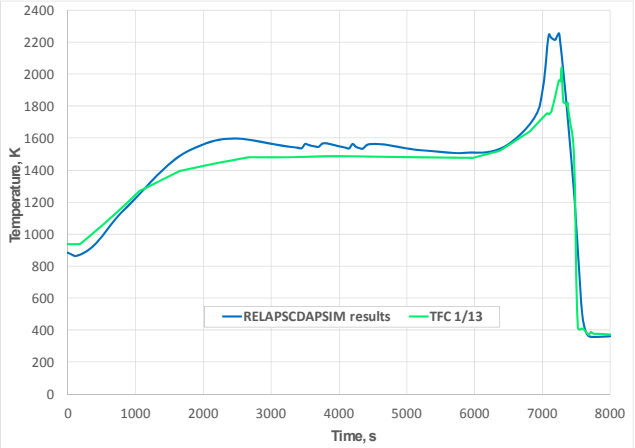

FIGURE 5. Time history of the measured and calculated inner unheated rod central temperature at elevation 950 mm

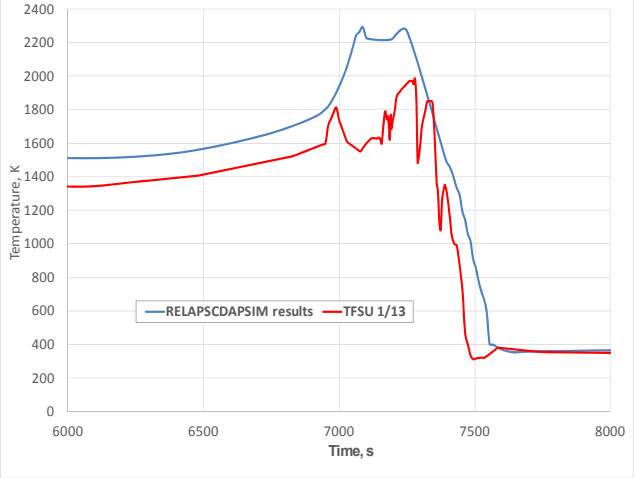

FIGURE 6. Time history of the measured and calculated inner unheated rod surface temperature at elevation 950 mm

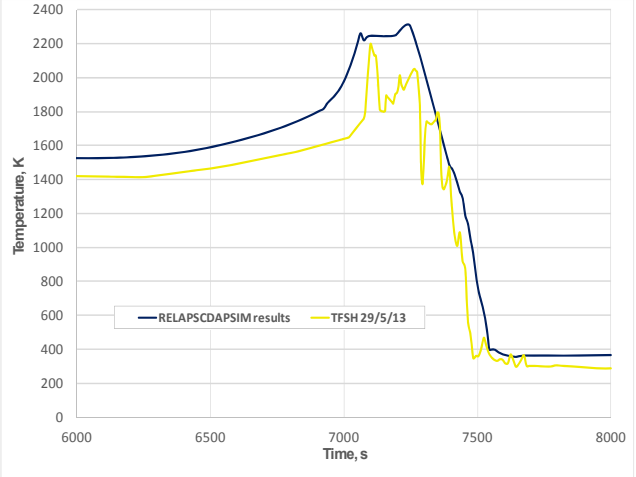

FIGURE 7. Time history of the measured and calculated outer heater rod cladding surface temperature at elevation 950 mm

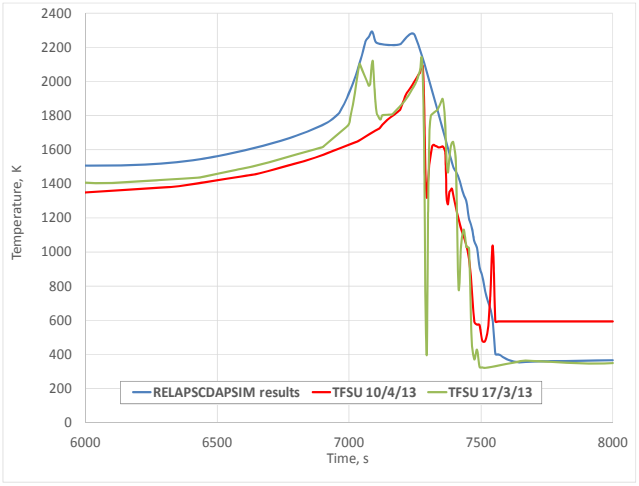

FIGURE 8. Time history of the measured and calculated outer unheated rod surface temperature at elevation 950 mm

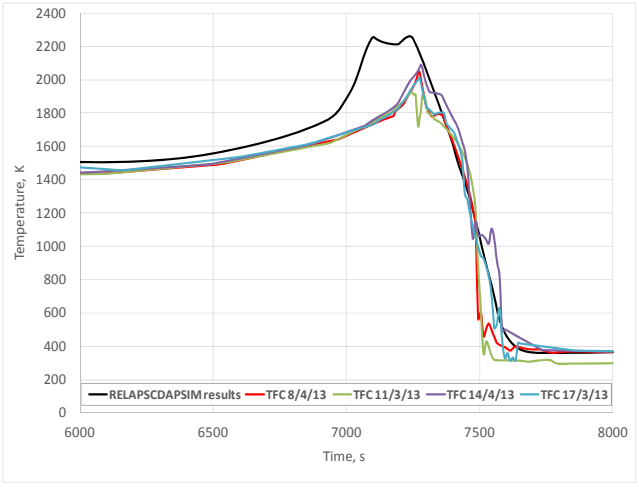

FIGURE 9. Time history of the measured and calculated central line unheated rod temperature at elevation 950 mm

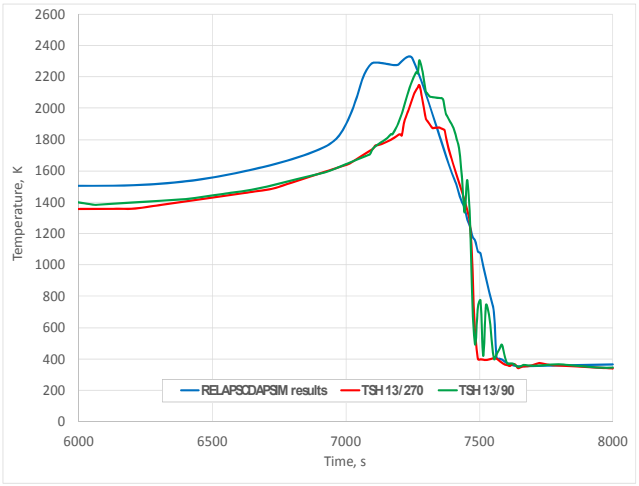

FIGURE 10. Comparison between the measured and calculated shroud surface temperature at elevation 950 mm

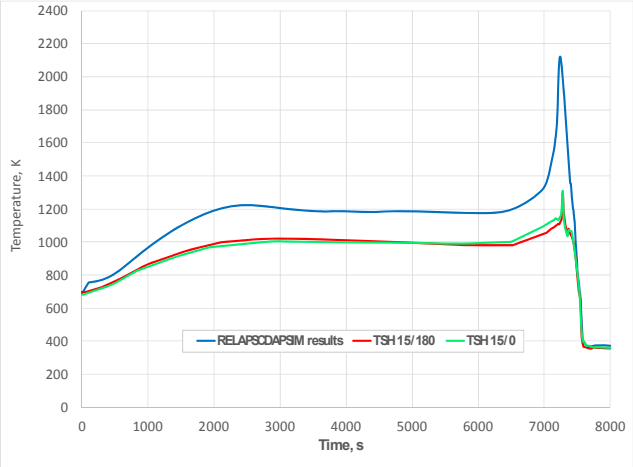

FIGURE 11. Time history of the shroud surface temperature at elevation 1150 mm

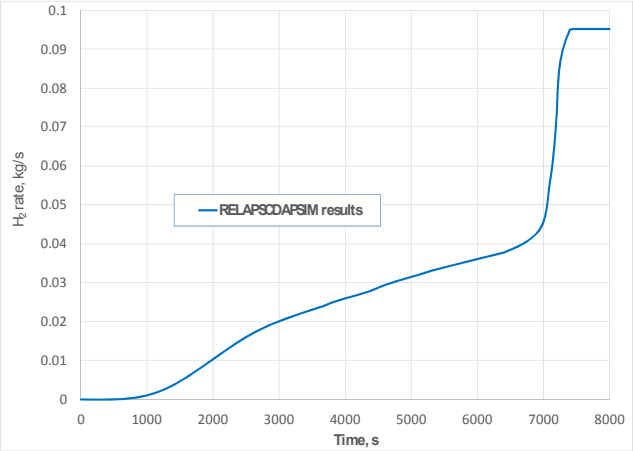

FIGURE 12. QUENCH 12: Integral hydrogen production

CONCLUSIONS AND OUTLOOK

The RELAP/SCDAP/MOD3.5 model of the QUENCH-12 experiment using the "*wolfhn*" heater rod is created and tested. It is validated against measured data. The numerical model, which is solved by using an automatic time advancement option, predicts results which are in good agreement with the experimental data. It reproduces qualitatively the measured data during all phases of the experiment. The bundle temperatures during the pre-oxidation phase are over predicted. Up to elevation 750 mm, the maximal deviation between the predicted and measured bundle temperatures during the transient phase is about 100 ˚C. The temperature difference increases with the height of the test bundle, as in elevation 950 mm it reaches about 310 ˚C.

A larger area of shroud melting is predicted. It covers the bundle section up to elevation 1150 mm.

The model overestimates the measured hydrogen by 64%, as gives integral hydrogen production equal to 92 grams.

The subject of future work is the study of the numerical uncertainty of different axial and radial discretization, as well as the used numerical methods.

ACKNOWLEDGMENTS

This research is partially supported by project *Stochastic project and simulation models in the field of medicine, social sciences and dynamic systems* funded by the National Science Fund of Ministry of Education and Science of Bulgaria (Contract No. DN12/11/20. Dec. 2017).

REFERENCES

1. J. Stuckert, A. Goryachev, M. Große, M. Heck, I. Ivanova, G. Schanz, L. Sepold, U. Stegmaier, M. Steinbrück, Results of the QUENCH-12 Experiment on Reflood of a VVER-Type Bundle, KIT SCIENTIFIC REPORTS FZKA 7307, 2008, Available from: http://quench.forschung.kit.edu/
2. L. Sepold, P. Hofmann, W. Leiling, A. Miassoedov, D. Piel, L. Schmidt, M. Steinbrück, Reflooding Experiments with LWR-Type Fuel Rod Simulators in the QUENCH Facility, Nuclear Engineering and Design 204 (2001) 205–220, Available from: https://www.sciencedirect.com
3. S. Sadek, S. Spalj, and D. Grgic, RELAP5/SCDAPSIM analysis of the QUENCH-06 experiment, FER-ZVNE/SA/DA-IR01/03-0, Zagreb, 2003
4. M. Steinbrück, M. Große, L. Sepold, J. Stuckert, Synopsis and Outcome of the QUENCH Experimental Program, Nuclear Engineering and Design 240 (2010) 1714–1727, Available from: https://www.sciencedirect.com
5. H. Kim, I. Kim, B. Choi, J. Park, A Study of the Breakaway Oxidation Behavior of Zirconium Cladding Materials, Journal of Nuclear Materials 418 (2011) 186–197, Available from: https://www.sciencedirect.com
6. M. Négyesi, J. Burda, V. Klouček, J. Lorinčík, J. Sopoušek, J. Kabátová, L. Novotný, S. Linhart, T. Chmela, J. Siegl, V. Vrtílková, Contribution to the Study of the Pseudobinary Zr1Nb–Oxygen Phase Diagram by Local Oxygen Measurements of Zr1Nb Fuel Cladding After High Temperature Oxidation, Journal of Nuclear Materials 420 (2012) 314–319, Available from: https://www.sciencedirect.com
7. Z. Hózer, C. Győri, L. Matus, M. Horváth, Ductile-to-brittle Transition of Oxidized Zircaloy-4 and E110 Claddings, Journal of Nuclear Materials 373 (2008) 415–423
8. I. Vetvicka, Effect of Creep and a-Zr ↔ (α + β)-Zr Transition in Zr1Nb Cladding on Texture Analyzed by Neutron Diffraction, Journal of Nuclear Materials 453 (2014) 196–201
9. E. Perez-Feró, C. Győri, L. Matus, L. Vasáros, Z. Hózer, P. Windberg, L. Maróti, M. Horváth, I. Nagy, A. Pintér-Csordás, T. Novotny, Experimental Database of E110 Claddings Exposed to Accident Conditions, Journal of Nuclear Materials 397 (2010) 48–54, Available from: https://www.sciencedirect.com
10. E. Perez-Feró, T. Novotny, A. Pintér-Csordás, M. Kunstár, Z. Hózer, M. Horváth, L. Matus, Experimental Results on the Breakaway Oxidation of the E110 Cladding Alloy Under High-Temperature Isothermal Conditions, Progress in Nuclear Energy 93 (2016) 89–95, Available from: https://www.sciencedirect.com
11. M. Steinbrück, N. Vér, M. Große, Oxidation of Advanced Zirconium Cladding Alloys in Steam at Temperatures in the Range of 600–1200 °C, Oxidation of Metals, Vol. 76, Issue 3-4, 215–232, 2011, Available from: https://link.springer.com
12. A. Stefanova, P. Groudev, Simulation of Quench-12 Test with ASTEC1.3.2 Computer Code, SOP Transactions on Applied Physics, Volume 1, Number 2, June 2014
13. L. Sepold, M. Steinbrück, J.Stuckert, A.Goryachev, VVER Bundle Test QUENCH-12 Quick Look Report, Interner Bericht, 32.22.11 NUKLEAR 3410
14. J. Stuckert, L. Sepold, M. Steinbrück, Results of the QUENCH-12 Experiment on Reflood of a VVER-Type Bundle, 15th International Conference on Nuclear Engineering, Nagoya, Japan, April 22-26, 2007, ICONE15-10257
15. H. Madokoro, N. Erkan, K. Okamoto, Assessment of the models in RELAP/SCDAPSIM with QUENCH-06 analysis, Journal of Nuclear Science and Technology, Volume 52, 2015 - Issue 11, Available from: https://www.tandfonline.com
16. W. Hering, Ch. Homann, Improvement of the SCDAP/RELAP5 Code with Respect to FZK Experimental Facilities, KIT SCIENTIFIC REPORTS FZKA 6566, 2007, Available from: https://publikationen.bibliothek.kit.edu/270068455
17. Y. Georgiev, J. Stuckert, Analysis of the QUENCH-12 Bundle Experiment with the ATHLET-CD2.2A Code, KIT SCIENTIFIC REPORTS 7622, 2012, Available from: http://quench.forschung.kit.edu/

18. J. Stuckert, J. Birchley, M. Große, T. Haste, L. Sepold, M. Steinbrück, Experimental and Post-Test Calculation Results of the Integral Reflood test QUENCH-12 with a VVER-type Bundle, Annals of Nuclear Energy 36 (2009) 183–192
19. J. Stuckert, M. Große, M. Steinbrück, Experimental and Post-Test Calculation Results of the Integral Reflood Test QUENCH-12 with a VVER-type Bundle, Computational and Experimental Studies of LWR Fuel Element Behavior Under Beyond Design Basis Accidents and Reflood Conditions: International Scientific and Technical Meeting, Moscow, Russia, July 27-28, 2009
20. M. Steinbrück, J. Birchley, A. Boldyrev, A. Goryachev, M. Grosse, T. Haste, Z. Hózer, A. Kisselev, V. Nalivaev, V. Semishkin, L. Sepold, J. Stuckert, N. Vér, M. Veshchunov, High-Temperature Oxidation and Quench Behaviour of Zircaloy-4 and E110 Cladding Alloys, Progress in Nuclear Energy 52, Issue 1 (2010) 19–36, Available from: https://www.sciencedirect.com
21. L. Sepold,W. Hering, C. Homann, A. Miassoedov, G. Schanz, U. Stegmaier, M. Steinbrück, H. Steiner, J. Stuckert, Experimental and Computational Results of the QUENCH-06 Test (OECD ISP-45). Scientific report FZKA-6664, Karlsruhe, February 2004; Available from: http://quench.forschung.kit.edu/
22. L. Sepold, W. Hering, G. Schanz, W. Scholtyssek, M. Steinbrück, J. Stuckert, Severe Fuel Damage Experiments Performed in the QUENCH Facility with 21-rod Bundles of LWR-Type, Nuclear Engineering and Design 237 (2007) 2157–2164, Available from: https://www.sciencedirect.com
23. J. Stuckert, J. Birchley, M. Große, T. Haste, L. Sepold, M. Steinbrück, Experimental and Post-Test Calculation Results of the Integral Reflood Test QUENCH-12 with a VVER-Type Bundle, Proceedings of ICAPP '08, Anaheim, CA USA, June 8-12, 2008, Paper 8116
24. T. Kaliatka, A. Kaliatka, V. Vileiniškis, E. Ušpuras, Modelling of QUENCH-03 and QUENCH-06 Experiments Using RELAP/SCDAPSIM and ASTEC Codes, Science and Technology of Nuclear Installations, Volume 2014, Article ID 849480, Available from: https://www.hindawi.com
25. M. Steinbrück, M. Große, L. Sepold, J. Stuckert, Lessons Learned from the QUENCH Programme at FZK, 15th International QUENCH Workshop, Karlsruhe Institute of Technology, 3-5 November 2009
26. T. Kaliatka, E. Ušpuras, A. Kaliatka, Modeling of QUENCH 03 and QUENCH 06 Experiments Using RELAP/SCDAPSIM Code, Proceedings of the 21th International Conference on Nuclear Engineering ICONE21, ASME, Chengdu, China, Article ID 15894
27. T. Ikeda, K. Katsuragi, N. Shirakawa, Analysis of International Standard Problem No. 45, QUENCH06 Test at FZK by Detailed Severe Accidents Analysis Code, IMPACT/SAMPSON, Journal of Nuclear Science and Technology, Vol. 40, Issue 4, p. 246–255, April 2003, Available from: https://www.tandfonline.com
28. T. Kaliatka, A. Kaliatka, V. Vileiniskis, Application of Best Estimate Approach for Modelling of QUENCH-03 and QUENCH-06 Experiments, Nuclear Engineering and Technology 48, Issue2, 419-433 (2016), Available from: https://www.sciencedirect.com
29. C. Allison, L. Siefken, J. Hohorst, J. Birchley, Recent Improvements in RELAP/SCDAPSIM/MOD3.4 Resulting from QUENCH and PARAMETER Bundle Heating and Quenching Experiments, Proceeding and Book of Abstracts of 8th International Conference on Nuclear Option is Countries with Small and Medium Electricity Grids, May 16-20, 2010, Dubrovnik, Croatia, p.75
30. Allison C.M., Hohorst J.K., Role of RELAP/SCDAPSIM in Nuclear Safety, Science and Technology of Nuclear Installations Volume 2010: Article ID 425658; Available from: http://dx.doi.org/10.1155/2010/425658
31. A. K. Trivedia, C. Allison, A. Khanna, P. Munshi, RELAP5/SCDAPSIM/MOD3.5 Analysis of the Influence of Water Addition During a Core Isolation Event in a BWR, Nuclear Engineering and Design 273 (2014) 298-303, Available from: https://www.sciencedirect.com
32. J. H. Spencer, D. Novog, J. K. Hohorst, C. M. Allison, Assessment of New Modeling in RELAP/SCDAPSIM/MOD 3.5 Using Experimental Results from the Quench Program, Proceedings of International Congress on Advances in Nuclear Power Plants (ICAPP'11), Nice, France, May 2-5, 2011, Paper 11081,
33. RELAP5/MOD3.3 Code Manual Volume I: Code Structure, System Models, and Solution Methods, Nuclear Safety Analysis Division December 2001 Information Systems Laboratories, Inc. Rockville, Maryland, Idaho Falls, Idaho
34. V. Vileiniškis, T. Kaliatka, A. Kaliatka, E. Ušpuras,A. Šutas, Uncertainty and Sensitivity Analysis of QUENCH Experiments Using ASTEC and RELAP/SCDAPSIM Codes, 10th International Topical Meeting on Nuclear Thermal-Hydraulics, Operation and Safety (NUTHOS-10), Okinawa, Japan, December 14-18, 2014
35. J. Hohorst, RELAP/SCDAPSIM Input Manual MOD 3.4 3.5 & 4.0, 2012

36. I. I. Petrova, B. N. Samsonov, V. E. Peletsky, A. V. Nikulina, N. B. Sokolov, L. N. Andreeva-Andrievskaya, Thermophysical Properties of Zirconium Alloy E110 (Zr-0.01Nb) after oxidation in air atmosphere, International Joutnal of Thermophysics, Vol.23, Issue 5, pp 1347–1358, 2002, Available from: https://link.springer.com
37. C. Allison, B. T. Le, G. Gerova, I. Spasov, M. Perez-Ferragut, J. Hohorst, QUENCH-06 experiment post-test calculations and integrated uncertainty analysis with RELAP/SCDAPSIM/MOD3.4 and MOD3.5, Proceedings of the 26th International Conference on Nuclear Engineering (ICONE' 18), Hamersmith, London, England, July 22-26, 2018, Paper 81912 (in press).